A *Saccharomyces cerevisiae* mutant strain defective in acetyl-CoA carboxylase arrests at the G$_2$/M phase of the cell cycle

Walid Al-Feel, James C. DeMar, and Salih J. Wakil*

Verna and Marrs McLean Department of Biochemistry and Molecular Biology, Baylor College of Medicine, Houston, TX 77030

To elucidate the essential functions of acetyl-CoA carboxylase (ACC1/FAS3) in *Saccharomyces cerevisiae*, a temperature-sensitive mutant (*acc1^{ts}*) was constructed. When the acc1^{ts} cells were synchronized in G$_1$ phase with α-factor at the permissive temperature of 24°C and then released from the blockade and incubated at the restrictive temperature of 37°C, 95% of the cell population became arrested at the G$_2$/M phase of the cell cycle despite the presence of fatty acids (C$_{14}$-C$_{26}$) in the medium. These cells developed large undivided nuclei, and the spindles of the arrested mutant cells were short. Shifting the G$_2$ arrested cells back to the permissive temperature resulted in a reversal of the cell-cycle arrest, with cells initiating mitosis. However, after 3 h of incubation at 37°C, G$_2$ arrested mutant cells lost viability and displayed a uniquely altered nuclear envelope. Using [1-^{14}C]acetate as a precursor for fatty acids synthesis, we identified the phospholipids and sphingolipids derived from acc1^{ts} cells and wild-type cells at 24°C and 37°C, respectively. The levels of inositol-ceramides [IPC, MIPC, and M(IP)$_2$C] and very long-chain fatty acids C$_{24}$ and C$_{26}$ declined sharply in the G$_2$/M arrested cells because of ACC inactivation. Shifting the acc1^{ts} cells to 24°C after 2 h of incubation at 37°C resulted in reactivation of the ACC and elevation of the ceramides and very long-chain fatty acid syntheses with normal cell-cycle progression. In contrast, synthesis of wild-type inositol-ceramides, C$_{24}$ and C$_{26}$, fatty acids were elevated on incubation at 37°C and declined when the cells shifted to the permissive temperature of 24°C.

ACC1 | VLCF | very long-chain fatty acid

Acetyl-CoA carboxylase (ACC1), a biotin-containing enzyme, catalyzes the carboxylation of acetyl-CoA to form malonyl-CoA, a key intermediate in the synthesis and metabolism of fatty acids. Malonyl-CoA is a donor of the C$_2$ units for not only the *de novo* synthesis of long-chain fatty acids and their elongation to very long-chain acids, but also for the synthesis of polyketides (1–7). In eukaryotes, including the yeast *Saccharomyces cerevisiae*, the carboxylase protein is a multifunctional polypeptide consisting of two catalytic domains, the biotin carboxylase and the transcarboxylase and the biotin-binding site of the carboxyl carrier protein domain. The genomic DNA coding for the yeast gene has been sequenced, and the predicted amino acid sequences show high similarity to animal ACC1 (8). Antibodies against the yeast ACC1 cross-react with the ACC1 from animal sources, indicating high structural conservation.

Like other eukaryotes, yeast membrane lipids consist primarily of phospholipids, sphingolipids, and sterols. The fatty acid components of these lipids vary considerably in their chain lengths. The long-chain fatty acids (C$_{14}$, C$_{16}$, and C$_{18}$) are essential for yeast growth and viability and are synthesized *de novo* from acetyl-CoA and malonyl-CoA, reactions catalyzed by the multifunctional complex, $\alpha_{6}\beta_{6}$, fatty acid synthase (1, 9) or by elongation of myristoyl C$_{14}$-CoA to palmitoyl C$_{16}$-CoA by using the fatty acid elongation system *EL01* (2). Other elongation systems, *ELO2* and *ELO3*, that are required for the formation of very long-chain fatty acids up to C$_{24}$ (catalyzed by *ELO2*)

and its further elongation to C$_{26}$ (catalyzed by *ELO3*) are essential for the growth of yeast. Mutations of either gene produce pleotropic effects involving many membrane functions. However, disruption of both *ELO2* and *ELO3* genes produces a lethal phenotype yeast (2). Malonyl-CoA, generated by the carboxylase, is the key intermediate in the synthesis of long-chain and very long-chain fatty acids, which are the hydrophobic components of membrane lipids. Hence, the acetyl-CoA carboxylase (*ACC1/FAS3*) gene is essential for the growth and viability of the yeast cells, as was shown independently by Al-Feel *et al.* (10) and Hasslacher *et al.* (11). Supplementation of the media with fatty acids of various chain lengths failed to support the growth of yeast *acc1* null mutants. This may possibly be due to the requirement of very long-chain fatty acids or derivatives thereof, that are generated *in situ* and utilized in the synthesis of specific membrane lipids.

In general, the very long-chain fatty acids produced by the elongation systems become components of sphingolipids (12–14). In yeast, sphingolipids have diverse roles that include signal transduction during heat stress response, regulation of cell cycle, trafficking of vesicles from endoplasmic reticulum to the Golgi apparatus, and as component lipids in the glycosylphosphatidylinositol anchored protein (15, 16). In higher eukaryotes, ceramides play important roles in cell cycle, apoptosis, and cell senescence (15). Several studies have shown that the turnover of membrane phospholipids, especially phosphatidylcholine, is high during the G$_1$ phase of the cell cycle (17) and that they accumulate during the S phase (18). There is very little information regarding phospholipid metabolism during the G$_2$ and M phases (19). Several studies of the cell cycle have suggested that phospholipid synthesis is highly regulated and well integrated within the pathways involved in cell division (20). However, the precise biochemical mechanisms remain obscure.

Numerous studies of DNA replication, DNA repair, and chromosomal segregation (21) during the cell cycle, primarily in yeast, have disclosed the existence of cell-cycle checkpoints and feedback controls that assure proper replication and segregation of chromosomes. In eukaryotes, detailed studies concerning the requirement of accurate membrane synthesis for successful cell-cycle completion are lacking. Herein, we demonstrate that inactivation of the ACC1 protein in *S. cerevisiae* resulted in a cell-cycle arrest in G$_2$ despite the presence of long and very long-chain fatty acids in the culture medium.

Materials and Methods

Yeast Strains. Yeast strain Y202 (*MAT a, can1-100, ade2-1, his3-11,15, leu2-3,112, trp1-1, ura3Δ100*) was used to construct the temperature-sensitive mutant strain *acc1^{ts}* (*MAT a, can1-100, ade2-1, his3-11,15, leu2-3,112, trp1-1, ura3Δ100; acc1:: URA,*

---

pUN100-acc). The yeast was grown at 24°C and maintained in yeast extract/peptone/dextrose (YPD) medium (Difco) containing 1% yeast extract and 2% Bacto-peptone with 2% glucose as a carbon source. The strains were then transferred to complete synthetic medium (SD, Difco) containing yeast nitrogen base and vitamins. Various amino acids were added as needed (22). In culture media that were supplemented with exogenous fatty acids, the concentrations of the acids used were 0.001% (wt/vol) each of myristate, oleate, elaidate, arachidate, liganoserate, and hexacosanate; 0.0025% stearate; 0.0035% palmitate; and 0.0001% behenate. Ergosterol was added at 15 μg/ml. Phytosphingosine supplementation was 0.001% in Tween 40 (1% wt/vol).

Synchronization of Yeast Cells at the G_1 Phase. Yeast cells were grown in YPD culture media (pH 3.9) or YPD cultures containing fatty acids (YPD + FA) to the early log phase and were arrested at the G_1 phase by adding α-factor, the yeast mating pheromone, to a final concentration of 5 μg/ml. After incubation at 24°C for 3 h, the G_1-arrested cells were collected, washed twice with YPD medium, and resuspended in the same medium and incubated at 37°C for 2 h. Every 30 min, cell samples (1 ml) were withdrawn and fixed with either 70% ethanol or 3.7% formaldehyde and stored, respectively, at −20°C and 4°C.

Microscopic and Flow Cytometric Analyses. The ethanol-fixed cells were isolated by centrifugation, washed twice with PBS, and resuspended in PBS. To visualize the DNA, the cells were stained with 1 μg/ml 4,6-diamidino-2-phenylindole (DAPI). To visualize the microtubules, the formaldehyde-fixed cells were incubated with rat antitubulin monoclonal antibody YOL1/34 and FITC-conjugated secondary antibody (23). To measure the DNA content, ethanol-fixed cells were stained with propidium iodide (24) and analyzed using an EPICS model 753 Laser System flow cytometer.

For electron microscopic analysis, cultured cells were fixed in 2% glutaraldehyde in 40 mM phosphate buffer (pH 6.5) containing 0.5 mM MgCl$_2$ and embedded and stained as described (23).

Incorporation of [^{14}C]Acetate into Lipids. Yeast cells (*acc1*^{ts}) were grown at 24°C to the early log phase (OD$_{600}$ = 0.4) in YPD medium (pH 3.9), and α-factor was added to a final concentration of 5 μg/ml to arrest the cells in the G_1 phase. The cells were then washed twice with YPD medium, resuspended in the same medium, and incubated at 37°C for 2.5 h. Every 30 min, 1 ml was withdrawn and 1 μCi of [1-^{14}C]acetate (59.5 mCi/mmol, ICN; 1 Ci = 37 GBq) was added, and the mixture was incubated at 37°C for 10 min. Samples (0.01 ml) were withdrawn, and the cells were spread on a Millipore filter and washed with cold 5% trichloroacetic acid containing 0.01% acetate; their radiolabeling was then measured in a liquid scintillation counter. The remaining cells were harvested, and the lipids were extracted as described by Angus and Lester (25). The solvents were then removed under nitrogen gas, and the lipids were dissolved in methanol. A sample was withdrawn, and the lipids were analyzed on Silica Gel 60 high performance TLC plates (Merck) (26). The radiolabeled phospholipids and neutral lipids were identified by autoradiography.

For the incorporation of [^{14}C]acetate into the ceramides, separate experiments were carried out in which *acc1*^{ts} and wild-type yeast were arrested at 37°C for 2 h in the presence of 1 μCi/ml [1-^{14}C]acetate. The total lipids were extracted as above, and the radiolabeled ceramides were determined after mild alkaline methanolysis using 0.5 ml of monomethylamine and incubation at 52°C for 30 min (27). The reaction mixture was dried under nitrogen, and the residue was dissolved with chloroform:methanol:water (16:16:5) and analyzed on Silica Gel 60 high performance TLC plates. Alkaline-stable lipids and total
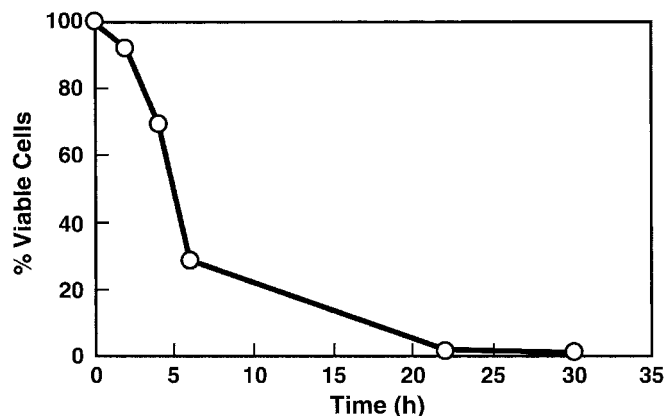

Fig. 1. Viability of acc1^{ts} yeast at 37°C. Cells harboring the pUN100-acc plasmid (acc1^{ts}) were grown at 24°C in 10 ml of YPD to an optical density of 0.4 at 600 nm, then shifted to 37°C. At the indicated time, a sample was withdrawn, plated onto YPD plates, and incubated at 24°C. The percentages of viable cells were calculated based on the number of colonies formed on the plates relative to the total number of cells as determined by a Coulter counter.

lipids were separated using a single-dimension solvent system of chloroform:methanol:4.2 N NH$_4$OH (9:7:2). The radiolabeled lipids were identified by autoradiography. In a separate experiment, the procedure was repeated using either *myo*-[2-^{3}H]inositol or [U-^{14}C]mannose to label the yeast cells and their respective ceramides, inositol-phosphorylceramide (IPC), mannose-inositol-P-ceramide (MIPC), and mannose-(inositol-P)$_2$-ceramide [M(IP)$_2$C].

Analyses of the Fatty Acids of the Ceramides. Employing the Hachey *et al.* procedure (28), the ceramides were saponified for 60 min at 80°C in 15% (wt/vol) KOH in methanol. The hydrolysates were diluted with H$_2$O, acidified, and extracted with hexane. The dried fatty acid extracts were reacted for 60 min at 80°C with 1.3 parts (vol/vol) 0.26 M 2,3,4,5,6-pentafluorobenzyl bromide in methylene chloride and 0.1 M aqueous tetrabutylammonium hydrogen sulfate buffered to pH 8.0 with potassium phosphate. The pentafluorobenzyl esters were extracted with hexane, purified on silica gel column (Extract-Clean Silica, Alltech Associates) by using 96:4 (vol/vol) hexane/methyl *t*-butyl ether, and separated by gas chromatography on a 60-m SP-2380 capillary column (Supelco), using a Hewlett–Packard 5890 gas chromatograph. Detection of pentafluorobenzyl esters was carried out by mass spectrometry on a Hewlett–Packard 5989A quadrupole mass spectrometer. Signals for various fatty acids were determined under negative chemical ionization using selective ion monitoring for their corresponding natural molecular masses. Identifications were confirmed using standard pentafluorobenzyl esters.

Results

Cell Synchrony. The yeast mutant, *acc1*^{ts}, is a temperature-sensitive strain that exhibits normal growth and viability at 24°C but loses viability at 37°C within 8–10 h as shown in Fig. 1. Supplementing cell cultures of acc1^{ts} grown at 24°C with α-factor caused acc1^{ts} synchronized in G_1 phase. When the cells were then transferred to fresh medium devoid of α-factor and incubated at 37°C for 30 min, cell growth was halted, and 90% of the cell population was arrested as shown by fluorescence-activated cell sorting analysis (Fig. 2*A*). Incubation of these cells for an additional 90 min did not alter their viability nor their G_2 phase status. Further incubation of the cells at 37°C for an additional 3–12 h resulted in an irreversible loss of viability (data not shown). The addition of a mixture of long-chain fatty acids (C$_{14}$,
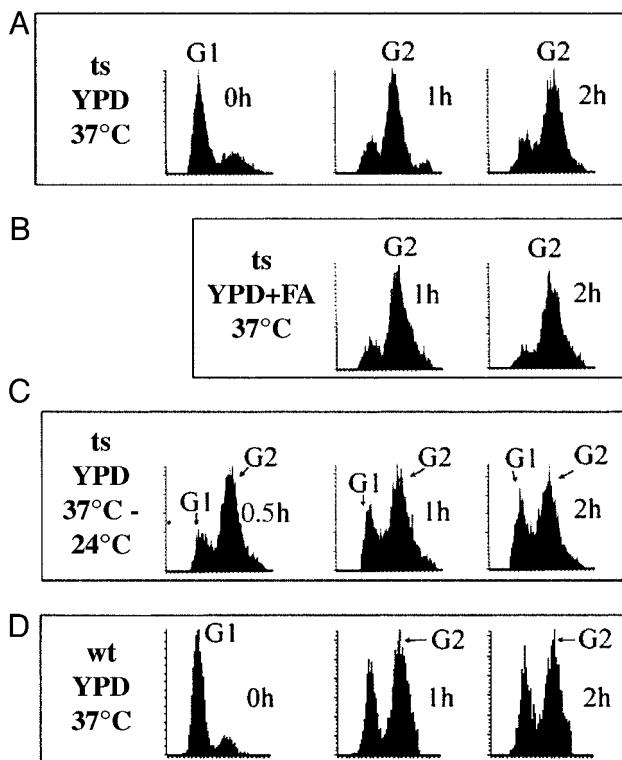
Fig. 2. Flow cytometric analyses of DNA contents of acc1[ts] mutant and wild-type yeast at 37°C. Cells were synchronized in G_1 with α-factor at 24°C, as described in *Materials and Methods*. (*A*) Cells were released into YPD media and incubated at 37°C. At the indicated times of incubation, samples were withdrawn and fixed with either 70% alcohol or 3.7% formaldehyde and placed, respectively, at −20°C and 4°C. Microscopic and flow cytometric analyses were carried out as described in *Materials and Methods*. (*B*) Same as in *A* plus fatty acids (in all combinations, see text). (*C*) acc1[ts] cells were synchronized at the G_2 phase by incubation for 2 h at 37°C, as described in *A*, then shifted to 24°C for 0.5, 1, and 2 h. (*D*) Wild-type yeast was synchronized with α-factor at 24°C and, after releasing into YPD, was incubated at 37°C. Samples were collected after 1 and 2 h and treated as in *A* and *B*. In each figure, the left-most peak represents the G_1 population and the right-most peak represents the G_2 population, as indicated.

C_{16}, and C_{18}) to the medium at 37°C did not overcome cell-cycle arrest (Fig. 2*B*); neither did the addition of very long-chain fatty acids (C_{20} to C_{26}) nor ergosterol, singularly or in combination with the long chain of fatty acid, overcome cell-cycle arrest or preserve cell viability after 3 h of incubation at 37°C. However, the mutant *acc1[ts]* cells, synchronized for 2 h at 37°C and then returned to 24°C, entered a new cell cycle as demonstrated by flow cytometric analysis of their DNA content (Fig. 2*C*). Wild-type yeast, on the other hand, when synchronized with α-factor at 24°C and released into YPD media at 37°C (with or without fatty acids), did carry out cell division as shown in Fig. 2*D*.

Phenotypic Studies of G_2 Phase-Arrested *acc1[ts]* Yeast. To better understand how a lack of functional *ACC1* affects the yeast cell cycle, we used fluorescence microscopy to examine the DAPI-stained DNA and antibody-stained microtubules in the arrested acc1[ts] cells and identified any phenotypic changes. When acc1[ts] cells arrested in the G_2 phase, followed by incubation at 37°C for 2 h and examined under the microscope, they showed unusually large budded cells (Fig. 3*A*) as compared with similarly treated wild-type cells (Fig. 3*C*). Moreover, compared with the normal nuclear morphology of wild-type cells (Fig. 3*C'*), most of the DAPI-stained *acc1[ts]* mutant cells had an abnormally large nucleus that resided in the mother cells (Fig. 3*A'*). Additionally,
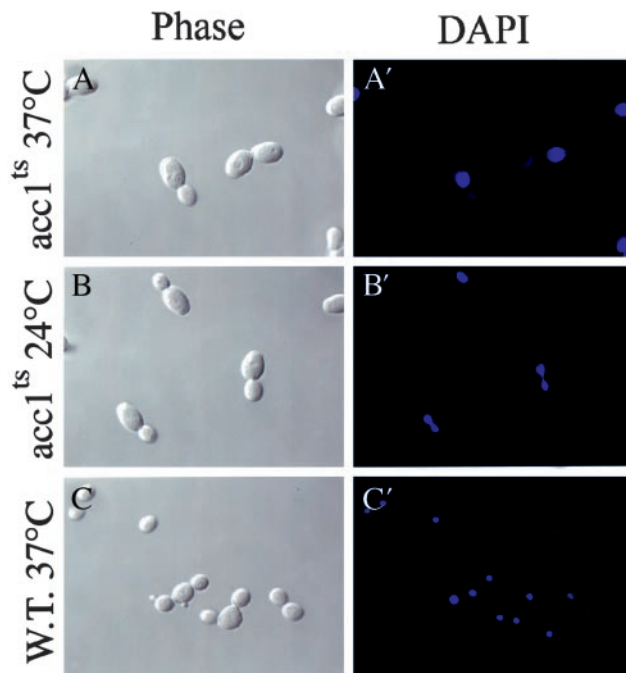
Fig. 3. Morphology of acc1[ts] and wild-type cells. Phase and immunofluorescence microscopy of acc1[ts] and wild-type cells were carried out as described in *Materials and Methods*. (*A*) Phase optics acc1[ts] cells were arrested at G_1 at 24°C by using α-factor and released in YPD and incubated at 37°C for 2 h. (*B*) After 2 h of incubation at 37°C, the acc1[ts] cells were shifted to 24°C, and samples were collected after 30 min and examined as in *A*. (*C*) The wild-type cells were treated and examined as in *A*. (*A'*–*C'*) The DNA of yeast nuclei of corresponding yeast strains used in *A*–*C* were stained with DAPI.

there were several mother cells that contained two small nuclei. When acc1[ts] cells, arrested in G_2 by incubation at 37°C for 2 h, were returned to 24°C, nuclear division resumed after 30 min, and the nuclear phenotypes of the G_2 phase-arrested acc1[ts] cells were normal (Fig. 3 *B* and *B'*).

Antitubulin antibody staining of the microtubules in both the *acc1[ts]* and wild-type cells showed that the mitotic spindles were shorter in the *acc1[ts]* cells than those formed in the wild-type cells after their arrest at the G_1 phase at 24°C, followed by their incubation at 37°C for 2 h (Fig. 4 *A* and *E*). The short mitotic spindles of the *acc1[ts]* mutant yeast arrested at G_2 (Fig. 4*A*) is the same as that of the known G_2-arrested cdc13–1 yeast cells (Fig. 4*C*) (29).

To determine whether there were any changes in the nuclear envelope phenotype of the G_2 phase-arrested *acc1[ts]* cells, we examined the cells under an electron microscope and showed that, within the first 3 h of incubation at 37°C, there were no visible changes (Fig. 5*A*). However, after 3.5 h of incubation at 37°C, we observed drastic changes including a separation between the inner and outer membranes of the nuclear envelope (Fig. 5*B*). Under these conditions, the cells had begun to lose viability (Fig. 1). We could not determine whether the altered nuclear envelope resulted from the loss of viability or was a secondary lethal effect or both.

Characterization of Total Lipids of acc1[ts] Cells. The incorporation of [1-^{14}C]acetate into the total lipids of the G_2 phase-arrested *acc1[ts]* cells within the first 2 h of incubation at 37°C was the same as that of the wild-type yeast cells as determined by pulse labeling every 30 min of incubation. However, after 3 h of incubation of the two cell lines at 37°C, there was seven times more incorporation of the [^{14}C]acetate into the total lipids of the wild-type than that of the *acc1[ts]* mutant yeast. Analysis of the total lipids
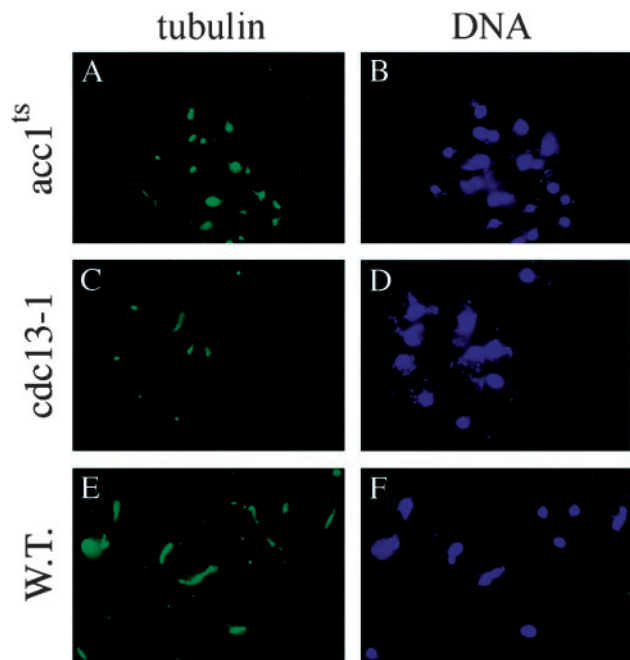
Fig. 4. The spindle structures and nuclear morphologies of acc1[ts] and wild-type cells. Indirect immunofluorescence measurements were obtained with anti-tubulin antibodies of acc1[ts], cdc13-1, and wild-type strains after their release into YPD from G_1 α-factor arrest at 24°C and incubation at 37°C for 2 h. (*A*) G_2 acc1[ts]-arrested cells exhibit short spindles. (*C*) As a control, the G_2 cdc13-1-arrested cells also displayed short spindles. (*E*) Wild-type yeast strain shows normal spindle structure morphology. (*B*, *D*, and *F*) Immuno-fluorescence microscopy of DAPI-stained nuclei of the corresponding yeast strains used in *A*, *C*, and *E*, respectively.

obtained after 2 h of incubation at 37°C showed that there was considerable and equal levels of incorporation of [1-^{14}C]acetate into the neutral and charged phospholipids (phosphatidylethanolamine, phosphatidylcholine, phosphatidylserine, and phosphatidylinositol) in both the *acc1*[ts] and wild-type cells (data not shown). However, the synthesis of sphingolipids was significantly reduced when *acc1*[ts] cells were arrested in the G_2 phase. The incorporation of [^{14}C]acetate into alkaline-stable lipids (27) obtained from *acc1*[ts] yeast was significantly lower than that of the
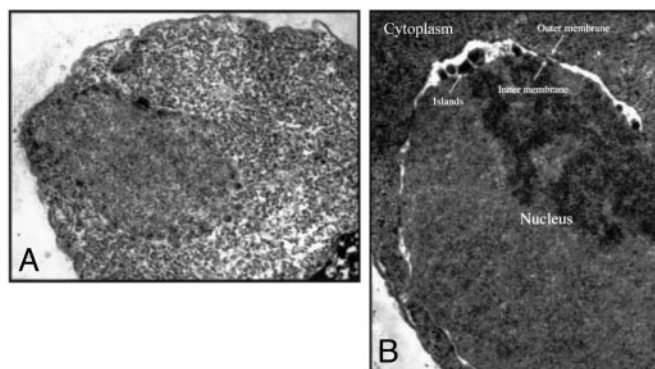

Fig. 5. Transmission electron microscopy of the nuclear envelope of acc1[ts] cells at a restrictive temperature for 1 h (*A*) and for 3.5 h (*B*). The acc1[ts] cells in *B* developed an altered nuclear envelope, which is defined by noncharacterized interspace between the outer and inner membrane of the nuclei, similar to the phenotype reported for the mtr7–1 yeast cells (30). The nuclear envelope of the wild-type yeast showed no changes when the cells were treated as in *B*. I, inner nuclear membrane; O, outer nuclear membrane; N, nucleus.
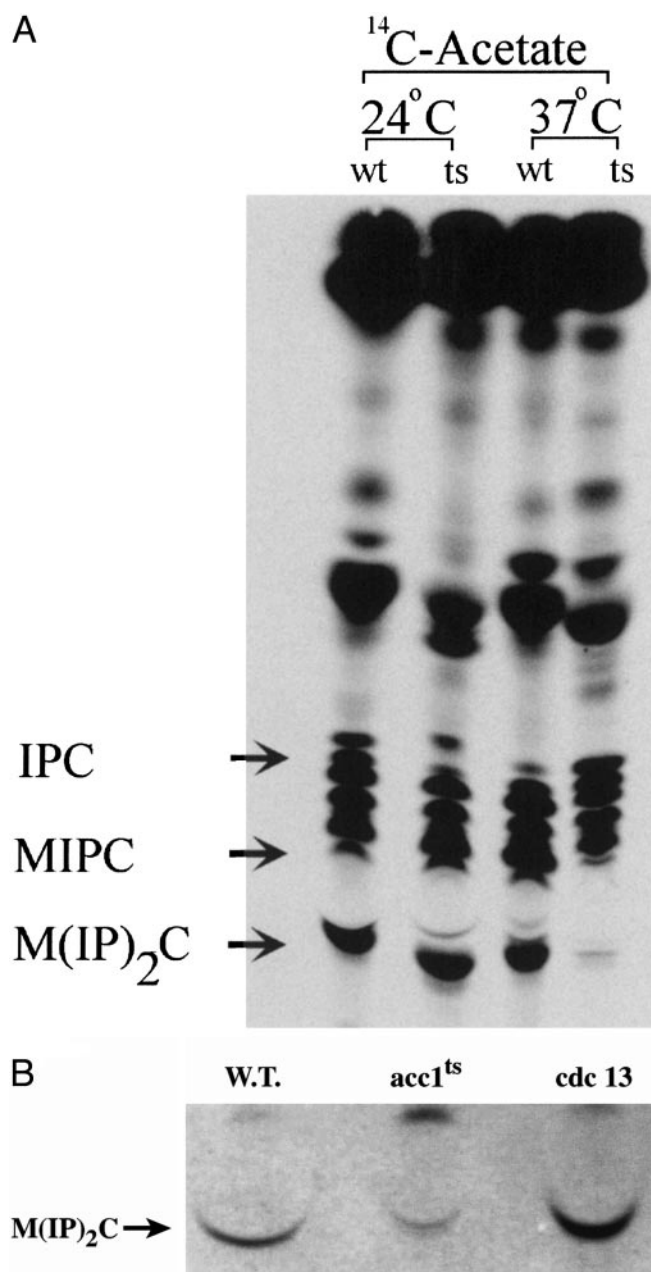
Fig. 6. Incorporation of [^{14}C]acetate into alkaline-stable lipids of acc1[ts] and wild-type yeast. (*A*) The acc1[ts] (ts) and wild-type (wt) yeast cells were arrested at G_1 with α-factor at 24°C and then released in YPD and incubated at 37°C for 2 h in the presence of [^{14}C]acetate. In a parallel experiment, comparable (ts and wt) cells were incubated at 37°C for 2 h, then shifted to 24°C and labeled with [^{14}C]acetate for 2 h. The cells were harvested, and the total lipids were extracted and subjected to monomethyl alkaline hydrolysis and analyzed as described in *Materials and Methods*. The major IPC, MIPC, and M(IP)$_2$C were identified by their R_f values and their respective ceramides were labeled with either [^{3}H]inositol or [^{14}C]mannose (27). (*B*) TLC analysis of [^{14}C]acetate-labeled lipids. The acc1[ts], wild-type, and cdc13–1 yeast cells were arrested at G_1 with α-factor, then released in YPD and inoculated at 37°C and labeled with [^{14}C]acetate for 2 h as in *A*. The cells were harvested, and the total lipids were extracted, subjected to monomethyl alkaline hydrolysis, and separated as described in *Materials and Methods*.

wild-type yeast. Analysis of these lipids by thin-layer chromatography showed that there is a significant reduction in the incorporation of [^{14}C]acetate into IPC, MIPC, and M(IP)$_2$C of the *acc1*[ts] mutant than those in the wild-type yeast (Fig. 6*A*).
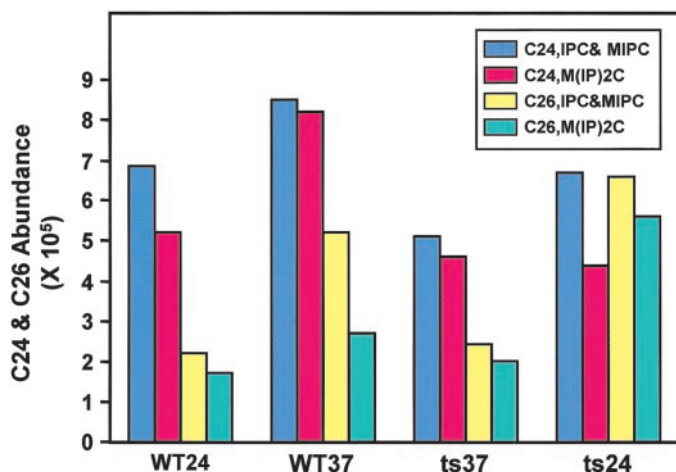
Fig. 7. GCMS analysis of IPC, MIPC, and M(IP)$_2$C fatty acids. The IPC, MIPC, and M(IP)$_2$C obtained from wild-type and acc1^{ts} strains labeled with [^{14}C]acetate at 37°C and 24°C as described in Fig. 6 were hydrolyzed, and the very long-chain fatty acids were extracted, purified, and subjected to mass spectroscopic analysis as described in *Materials and Methods*. The abundance of C$_{24}$ and C$_{26}$ was determined by GCMS analysis.

When the M(IP)$_2$C of the wild-type and *acc1*^{ts} grown at 37°C were eluted from the silica gel and their radiolabeling was measured, there was an ≈4.5-fold decrease in the radiolabeling of the M(IP)$_2$C of the *acc1*^{ts} mutant compared with that of the wild type. However, the incorporation of the [^{14}C]acetate into the M(IP)$_2$C of the two strains were the same when the cells were grown at 24°C as shown in Fig. 6*A*.

The difference in the incorporation of [^{14}C]acetate into the IPC, MIPC, and M(IP)$_2$C is not due to the arrest of the yeast at the G$_2$ phase of the cell cycle because the cdc13-1 yeast strain (a G$_2$ cell-cycle mutant) (29) expressing active ACC did not show differences in the incorporation of radioacetate into ceramides when grown at the restrictive temperature (Fig. 6*B*). Therefore, the arrest of the *acc1*^{ts} at the G$_2$ phase at the restrictive temperature is brought about by the loss of ACC activity at this temperature. Shifting the incubation temperature of the acc1^{ts} cells back to the permissive temperature of 24°C resulted in the reactivation of ACC and release from the cell-cycle block (Fig. 2).

Because ACC catalyzes the synthesis of malonyl-CoA (the donor of the C$_2$ units for the synthesis of long-chain and very long-chain fatty acids), we analyzed the abundance of the fatty acids, especially that of C$_{24}$ and C$_{26}$ of the IPC, MIPC, and M(IP)$_2$C derived from the acc1^{ts} mutant and wild-type yeasts (5, 30). The C$_{24}$ and C$_{26}$ fatty acid contents of the IPC and MIPC and the M(IP)$_2$C of the wild-type increased by 35–55% when the cells were shifted from 24 to 37°C (Fig. 7). This increase is in response to the stress encountered by the yeast cells due to their exposure to higher temperatures as reported by Hanun for animal and human cell lines (15). On the other hand, the C$_{24}$ and C$_{26}$ contents of the IPC and MIPC and the M(IP)$_2$C of the acc1^{ts} mutant cells were increased by ≈25%, 10%, 200%, and 180%, respectively, when the acc1^{ts} mutant cells were shifted back from 37°C to 24°C as shown in Fig. 7. This observation suggested that the availability of malonyl-CoA generated by the reactivated ACC1 may be preferentially used by *ELO3* for the synthesis of C$_{26}$ by the elongation of C$_{24}$ (2). There was also an increase in the abundance of C$_{24}$ in IPC and MIPC that too may have been synthesized by the elongation system as a result of ACC activation (Fig. 7).

Discussion

The requirement of acetyl-CoA carboxylase for the G$_2$/M to anaphase transition of ACC1^{ts} yeast mutant was hardly expected. The ACC1^{ts} cells arrested at 37°C were enlarged and developed large undivided nuclei (Fig. 3). Such enlargement of yeast cells has been shown to be a characteristic feature of most cdc mutants after prolonged cell-cycle arrest. It also indicates that in this state the cells continue to carry out active metabolism. Moreover, the G$_2$/M acc1^{ts}-arrested cells were still viable after 2 h at the restrictive temperature, as shown by their ability to recover and resume normal cell division when shifted to the permissive temperature of 24°C. Our analysis of these cells revealed that they had phenotypes that were consistent with that of most other G$_2$ phase-arrested yeasts, which have short spindles that were correctly oriented toward the bud, similar to the G$_2$-arrested cdc-13-1 yeast mutant. The G$_2$/M arrest suggests that a check point is censoring the absence of certain fatty acids or derivatives directly or indirectly.

Electron microscopy of the acc1^{ts} mutant cells arrested at the G$_2$ phase after incubation at 37°C for 3.5 h revealed considerable morphological changes in the nuclear membrane. As shown in Fig. 5, there were significant alterations in the nuclear membrane as shown by the separation of the outer and inner nuclear membrane and the presence of multiple vesicle islands within the newly generated interspaces. The nature of these morphological changes of the nuclear envelope is not known at this time. The expansion of the nuclear intermembrane space may account for loss of viability of the G$_2$-arrested acc1^{ts} yeast cells after a prolonged incubation at 37°C. In contrast, G$_2$-arrested acc1^{ts} cells incubated at 37°C for a shorter time period (<3.0 h) showed no apparent or irreversible changes in the nuclear membrane, which may explain why they could regain their cell-cycle status and pass through the G$_2$ phase to complete cell division after a lowering of the incubation temperature to 24°C.

Fatty acids are the apolar component of cellular lipid and are derived from food, synthesized *in situ* or a combination thereof. In yeast, malonyl-CoA, the product of acetyl-CoA carboxylase, is the key substrate in the synthesis of the fatty acid component of lipids, both cytoplasmic and nuclear. In eukaryotes, the lipid component of the nuclear envelope consists of phospholipids, with phosphatidylcholine and phosphatidylethanolamine being the major components and with phosphatidylserine and phosphatidylinositol as the minor components (5). Our evidence shows that the yeast nucleus also contains significant amounts of ceramides (data not shown). We expect that the synthesis of the fatty acid component of these lipids and ultimately the synthesis of viable nuclear membrane lipids are compromised in the viable G$_2$ phase-arrested acc1^{ts} cells and become more critical for the survival of the acc1^{ts} cells on prolonged incubation at 37°C. In support of this conclusion, we demonstrated that synthesis of total lipids, as measured by the incorporation of [^{14}C]acetate in the neutral and phospholipids, is not compromised in the G$_2$-arrested cells during the first 2 h of incubation of the *acc1*^{ts} mutant at 37°C. However, the incorporation of [^{14}C]acetate into these lipids declined sharply, and cells lost viability after incubation at 37°C for 3 h. In contrast, the radioactivity of the total lipids in the wild-type cells continued to increase on incubation at 37°C, and mitosis continued unperturbed.

The major difference in the absence of ACC1 is the reduction in ceramide contents of the cell. This is likely attributed to the lack of malonyl-CoA production in the *acc1*^{ts} mutant, because of inactivation of the carboxylase at 37°C and lack of malonyl-CoA for the synthesis of long and very long-chain fatty acids. Although the pathways for the biosynthesis of sphingolipids in yeast have been studied by Lester and Dickson (5), the enzymes and precise mechanisms involved have not been well established (16). In *S. cerevisiae*, sphingolipid accounts for 7–8% of the total

mass of the plasma membrane, as compared with the phospholipid contents of 30% of the plasma membrane consisting of phospholipid (5). The $M(IP)_2C$ content accounts for $\approx 75\%$ of the total sphingolipid, with IPC and MIPC comprising the rest (30). Their synthesis involves enzymes associated with the endoplasmic reticulum and the Golgi apparatus. Their cellular localization and functions, on the other hand, are not well understood. What distinguishes yeast ceramide from animal ceramide is the presence of an α-hydroxy-C_{26}-fatty acid coupled to the phytosphingosine. The synthesis of C_{26} involves the elongation systems, *EL02* and *EL03*, with malonyl-CoA generated by ACC1 providing the C_2 units (2, 3). However, the reaction sequences involved in the transacylation and hydroxylation reactions of the C_{26} fatty acid are currently unknown. The finding that addition of C_{24} and/or C_{26} to the acc1[ts] media did not support growth and viability suggests that these fatty acids may not be able to enter the cells or cannot be activated to the acyl substrate levels required in transacylation or hydroxylation reactions.

Analysis of the [^{14}C]acetate incorporated into the $M(IP)_2C$ derived from the G_2-synchronized acc1[ts] mutant incubated at 37°C for 2 h showed that there was a 4.5-fold decrease in radioactivity compared with that of the wild type treated in the same manner (Fig. 6*B*). The abundance of C_{24} fatty acids in the IPC and MIPC derived from the *acc1*[ts] mutant and wild-type yeasts grown at 24°C was the same (Fig. 7). When the G_1-synchronized acc1[ts] mutant cells were incubated at 37°C for 2 h, the abundance of C_{26} was ≈ 2.5-fold lower than that of IPC and MIPC isolated from the wild-type yeast treated in the same manner. When the temperature of incubation of acc1[ts] cells was returned to 24°C, there was a 3.5-fold increase in the synthesis of C_{26} over that for the wild-type cells at 24°C (Fig. 7). Similarly, the C_{26} contents of the IPC and MIPC of the acc1[ts] mutant after its return to 24°C was >3-fold higher than that of the wild-type C_{26} (Fig. 7). This increase is comparable and reflects the 4.5-fold increase in the incorporation of [^{14}C]acetate into the $M(IP)_2C$.

These results suggest that ACC is active at the permissive temperature and that the malonyl-CoA generated is preferentially used in the synthesis of C_{26}, which is then used in the synthesis of ceramides. The increased synthesis of ceramides [in this case, $M(IP)_2C$] of acc1[ts] cells during recovery from their arrest at G_2 indicates their essential role in the cell cycle. It is also possible that a low concentration of very long-chain fatty acids and ceramides in the arrested acc1[ts] cells affected the structure of the nuclear envelope in these cells, precluding its usual expansion during cell division.

The nuclear envelope is a major anchoring site for chromosomes during interphase and may play a key role in chromatin organization. As in higher eukaryotes, the nuclei of yeast cells in interphase contain mitotic spindles composed of microtubules. What distinguishes dividing yeast cells, however, is that the spindle pole bodies span the nuclear envelope, which remains visibly intact during the cell cycle (31). Many studies of cell division in higher eukaryotes have demonstrated a tight physical association between chromatin and the nuclear envelope (32). Our electron microscopy studies revealed dramatic changes in the morphology of the nuclear envelope after the G_2/M-arrested acc1[ts] mutant cells had lost viability after a 3.5-h incubation at 37°C. This may be due to changes in the ceramides, specifically $M(IP)_2C$ and possibly IPC and MIPC, and may have contributed to the occurrence of the *acc1*[ts] mutant cell-cycle arrest. This type of arrest may be another surveillance mechanism that responds to defects in nuclear envelope composition and architecture. Our results suggest that the synthesis of viable nuclear membrane plays a key role in the progression of cell division. Very long-chain fatty acid as components of sphingolipids contributes significantly to the structures of these lipids and their function in the mitotic division of the cell.

1. Wakil, S. J., Stoops, J. K. & Joshi, V. C. (1983) *Annu. Rev. Biochem.* **52,** 537–579.
2. Oh, C.-S., Toke, D. A., Mandala, S. & Martin, C. (1997) *J. Biol. Chem.* **272,** 17376–17384.
3. Toke, D. & Martin, C. (1996) *J. Biol. Chem.* **271,** 18413–18422.
4. Silver, S., Leplatois, P., Josse, A., Dupuy, P.-H., Lanau, C., Kaghad, M., Dhers, C., Rahier, A., Taton, M., Le Fur, G., *et al.* (1996) *Mol. Cell. Biol.* **16,** 2719–2727.
5. Lester, R. L. & Dickson, R. C. (1993) *Adv. Lipid Res.* **26,** 253–274.
6. Ahmad, P. & Ahmad, F. (1982) *Arch. Biochem. Biophys.* **220,** 557–562.
7. Munday, M. R., Campbell, D., Carling, D. & Hardie, D. (1988) *Eur. J. Biochem.* **175,** 331–338.
8. Al-Feel, W., Chirala, S. & Wakil, S. J. (1992) *Proc. Natl. Acad. Sci. USA* **89,** 4534–4538.
9. Lynen, F. (1980) *Eur. J. Biochem.* **112,** 431–442.
10. Al-Feel, W., Wakil, S. J. & Chirala, S. S. (1993) *FASEB J.* **7,** 1229.
11. Hasslacher, M., Ivessa, A. S., Paltauf, F. & Kholwein, S. D. (1993) *J. Biol. Chem.* **268,** 10946–10952.
12. Hechtberger, P., Zinser, E., Saf, R., Hummel, K., Paultauf, F. & Daum, G. (1994) *Eur. J. Biochem.* **225,** 641–649.
13. Patton, J. L. & Lester, R. L. (1992) *Arch. Biochem. Biophys.* **292,** 70–76.
14. Zweerink, M. M., Edison, A. M., Wells, G. B., Pinto, W. & Lester, R. L. (1992) *J. Biol. Chem.* **267,** 25032–25038.
15. Hannun, Y. A. (1996) *Science* **274,** 1855–1859.
16. Dickson, R. C. (1998) *Annu. Rev. Biochem.* **67,** 27–48.
17. Kyriakis, J. M. & Avruch, J. (1996) *J. Biol. Chem.* **271,** 24313–24316.
18. Fishbein, J. D., Dobrowsky, R. T., Bielawska, A., Garrett, S. & Hannun, Y. A. (1993) *J. Biol. Chem.* **268,** 9255–9261.
19. Jackowski, S. (1996) *J. Biol. Chem.* **271,** 20219–20222.
20. Al-Feel, W. & Wakil, S. J. (1997) *FASEB J.* **11,** 3117.
21. Newlon, C. S. (1988) *Microbiol. Rev.* **52,** 568–601.
22. Rose, M. D., Winston, F. & Hieter, P. (1990) *Methods in Yeast Genetics* (Cold Spring Harbor Lab. Press, Plainview, NY), p. 178.
23. Kilmartin, J. V. & Adams, A. E. M. (1984) *J. Cell Biol.* **98,** 922–933.
24. Hutter, K. J. & Eiple, H. E. (1979) *J. Gen. Microbiol.* **113,** 369–375.
25. Angus, W. W. & Lester, R. L. (1974) *Arch. Biochem.* **151,** 483–495.
26. Knoll, L. J. & Gordon, J. (1993) *J. Biol. Chem.* **266,** 4281–4290.
27. Clarke, N. G. & Dawson, R. M. C. (1981) *Biochem. J.* **195,** 301–306.
28. Hachey, D. L., Patterson, B. W., Reeds, P. J. & Elsas, L. J. (1991) *Anal. Chem.* **63,** 919–923.
29. Lydall, D. & Weinert, T. (1997) *Methods Enzymol.* **238,** 410–424.
30. Schneiter, R., Hitomi, M., Ivessa, A. S., Fasch, E.-V., Kohlwin, S. D. & Tortakoff, A. M. (1996) *Mol. Cell. Biol.* **16,** 7161–7172.
31. Byers, B. (1981) in *The Molecular Biology of the Yeast Saccharomyces: Life Cycle and Inheritance*, eds. Strathern, J. N., Jones, E. W. & Broach, J. R. (Cold Spring Harbor Lab. Press, Plainview, NY), pp. 59–96.
32. Grace, L. & Burke, B. (1988) *Annu. Rev. Cell Biol.* **4,** 335–374.